SUPPLEMENTARY MATERIALS

CONTENTS

DETAILED METHODS

Study Design

This was a single arm Phase 1/2 study (registered at ClinicalTrials.gov as NCT01165996). In MDS, morbidity and death is caused by low blood counts, and hematologic improvement (HI) produces better overall survival. HI or better was the primary end-point per International Working Group (IWG) 2006 Criteria for Response in MDS Clinical Trials, defined as an increase in hemoglobin of ≥1.5g/dL, reduction in red blood cell transfusion by at least 4 transfusions/8weeks compared with pre-treatment, increase in platelets by $\geq 30x10^9$/L (if baseline platelets $>20x10^9$/L), increase in platelets from $<20x10^9$/L to $>20x10^9$/L and by at least 100%, at least 100% increase in neutrophils and absolute increase $>0.5x10^9$/L (if baseline neutrophils $<0.5x10^9$/L). Secondary end-points included >Grade 2 toxicity by NCI/CTEP v4 criteria, measures of response and duration per IWG criteria, disease genetics by whole exome sequencing and standard metaphase karyotyping, and mechanism-of-action biomarker correlation with response.

Patients

Patients were enrolled after written informed consent on an Institutional Review Board approved protocol in accordance with the Declaration of Helsinki. A diagnosis of MDS classified by hematopathology review as WHO categories chronic myelomonocytic leukemia, atypical chronic myeloid leukemia (BCR-ABL1 negative), myelodysplastic/myeloproliferative neoplasm unclassifiable, refractory anemia with ring sideroblasts and thrombocytosis, refractory cytopenia with unilineage dysplasia, refractory anemia with ring sideroblasts, refractory cytopenia with multi-lineage dysplasia (RCMD), refractory anemia with excess blasts, myelodysplastic syndrome unclassifiable was required. In addition, subjects were required to have symptomatic anemia or thrombocytopenia with a platelet count of $<100 \times 10^9$/L, or transfusion dependence for red-cells, or transfusion dependence for platelets, or an absolute neutrophil count $<1 \times 10^9$/L. MDS with isolated del(5q) on cytogenetics was excluded unless failed prior lenalidomide therapy. Also excluded were individuals previously treated with decitabine, but not individuals previously treated with 5-azacytidine, lenalidomide or other therapies.

Other exclusion criteria were: (i) untreated erythropoietin deficiency defined as an erythropoietin level of <200 IU/L despite hemoglobin <9 g/dl, (ii) uncontrolled infection, (iii) severe sepsis or septic shock, (iv) current pregnancy or breast feeding, (v) the patient was of childbearing age, and is unwilling to use contraception and has not had a tubal ligation, hysterectomy, or vasectomy, or their partner is also unwilling to use an acceptable method of contraception as determined by the investigator, (vi) not able to give informed consent, (vii) altered mental status or uncontrolled seizure disorder, (viii) ALT >300 IU; or albumin < 2.0 mg/dL, (ix) creatinine > 2.5 mg/dl and creatinine clearance <60ml/min, (x) patients who were moribund or patients with concurrent hepatic, renal, cardiac, metabolic, or any disease of such severity that death within 60 days was likely, (xi) B12, folate, or iron deficient, until corrected, (xii) NYHA class III/IV status, (xiii) ECOG

performance status ≥3, (xiv) HIV positive or history of seropositivity for HIV, (xv) transformation to acute leukemia (≥ 20% myeloblasts in marrow aspirate).

Treatment

Study Drug and regimen (Fig 1): Study drug (Eisai, Tokyo, Japan), supplied as a lyophilized powder for injection (50mg), was reconstituted with 5ml sterile water to facilitate subcutaneous administration. If pre-treatment bone marrow myeloblast percentage was <10%, starting dose decitabine 0·2mg/kg was administered 2X/week for the initial 4 weeks (**Fig.1**). If bone marrow myeloblasts were ≥10% and there was a clinical concern of rapid progression to AML, the treating investigator had discretion to administer decitabine 0·2mg/kg 3X/week for 4 weeks. The planned duration of protocol therapy was 1 year (52 weeks).

Management of neutropenia: Neutrophil count nadirs occurring 5-8 weeks after initiation of therapy or after any increase in dose or treatment frequency were managed by temporary withholding of drug for 1-2 weeks and then resumption at the same dose or reducing the dose no more than 0.05mg/kg, with the minimum dose of 0.1mg/kg 1X/week. Granulocyte-colony stimulating factor (G-CSF) support was permitted if neutrophils were $<0.5x10^9$/L. The overall goal was to relieve cytopenia while maintaining malignant clone suppression with at least decitabine 0.1mg/kg 1X/week. Regular administration, at a lower dose if necessary, was always preferred to infrequent administration of a higher dose.

Bone marrow aspirate and biopsies: Worsening cytopenias concurrent with increasing bone marrow cellularity (hypercellular relapse) was an indication of progressive disease that could be managed with increasing frequency of drug administration (maximum 0.2 mg/kg 3X/week). Worsening peripheral cytopenias concurrent with a decrease in marrow cellularity (hypocellular relapse) could reflect nadir or over-treatment to be managed as described for neutropenia.

Immunohistochemistry

Immunostaining was performed on decalcified and formalin-fixed paraffin embedded bone marrow biopsy sections (4 μm) obtained at protocol screening (pre-treatment), weeks 6 and 12, and on positive and negative controls for each immunostain. Antibodies used were rabbit monoclonal antibody cMYC (clone Y69, Epitomics #1472-1, Burlingame, CA), 1:50 dilution for 1 hour at room temperature. Rabbit monoclonal antibody Ki67 (clone 30-9, Ventana Medical Systems, Inc. #790-4286, Tucson, AZ), predilute antibody for 16 minutes at 37 C^o. Both stains were performed with Ventana Benchmark Ultra using iView detection (Ventana #760-091) and a high pH tris-based buffer (Cell Conditioning 1, Ventana #950-124). Mouse monoclonal anti-p27 (clone Kip1, BD Bioscience #610241, CA), 1:1600 dilution for 32 minutes at room temperature. Mouse polyclonal anti-Dnmt1 (Abcam #ab19905, Cambridge, MA), 1:200 dilution for 32 minutes at room temperature. Both stains were performed with Ventana Discovery using OmniMap detection and a high pH tris-based buffer (Cell Conditioning 1, Ventana #950-124).

Image acquisition and quantitative immunohistochemical analysis

High resolution, large field-of-view images were acquired using a Leica SCN400 (Leica Microsystems Inc, Buffalo Grove, IL) at a scanning magnification equivalent to 20x (0.3 um/pixel). ImageIQ software (Image IQ Inc., Cleveland, OH) was used to manage and analyze whole section digital images. Using the ImageIQ software, it was possible to perform manual reviews of digital images in addition to automated image analysis (IA). The Image IQ automated image analysis algorithm was launched and implemented from within Image-Pro Plus software (Media Cybernetics, Silver Springs, MD) for batch analysis of all images. Analysis parameters were adjusted to detect cell nuclei. In brief, the algorithm used a combination of color detection and morphometric interpretation to isolate the nuclei that stained positive for the targeted biomarker (cMYC, Ki67, p27, and DNMT1) based on grayscale values. Whole tissue area was first calculated by converting images to grayscale and applying a low-pass filter followed by thresholding. Due to the similarity in hues to nuclei, bone within each section was segmented and "subtracted" from the original image using HSI color space conversion, image mathematical operations, and morphological "opening". For segmentation of positively stained nuclei (brown), the blue channel of the original RGB image was extracted, inverted, and segmented (intensity > 180, area > 10 pixels). A watershed filter followed by a morphological "opening" filter were applied to the resultant image to split touching nuclei. For segmentation negative nuclei (blue), a similar procedure was followed with the substitution of YIQ color space conversion for RGB channel extraction. Lastly, positive and negative cell counts, and tissue and bone areas were exported to Excel. Positively segmented nuclei Sobel filtered, pseudocolored green, and superimposed upon the original image for visual validation of the algorithm performance.

Flow Cytometry Quantification of γH2AX, a DNA Damage Marker

Bone marrow aspirate mononuclear cells were isolated using a standard density gradient procedure: ~6 mL of heparinized bone marrow aspirate was layered over an equal volume of Histopaque®-1077. Cells fixed with 1% paraformaldehyde (EMS grade Cat #15710) were permeabilized with cold methanol and blocked with 6% FBS for 15 minutes at room temperature prior to immunostaining with Alexa Fluor® 488-conjugated mouse anti-γH2AX (pS139, cat# 560445) for 1 hour at room temperature. Positive (BD Biosciences, cat #51-6552LZ) and negative control cells (Cat 51-6553LZ) as well as healthy donor cell controls were concurrently stained and analyzed. Flow cytometric analysis was performed with an FC500 flowcytometer (Beckman-Coulter Inc) equipped with CXP acquisition software (CXP analysis 2.2, Beckman Coulter Inc). Gating was determined by positive and negative controls, and results were expressed as the percentage of cells demonstrating fluorescence intensity located within this positive gate.

Whole Exome Sequencing

Sequencing procedures: Tumor DNA was extracted from bone marrow mononuclear cells. For germline control, DNA was obtained from paired CD3 positive T cells. Whole exome capture was accomplished based on liquid phase hybridization of sonicated genomic DNA having 150 - 200bp of mean length to the bait library synthesized on magnetic beads (SureSelect®, Agilent Technology), according to the manufacture's protocol (SureSelct Human All Exon 50Mb kit). The captured targets were subjected to massive sequencing using Illumina GAIIx and/or HiSeq 2000 with the pair end 75-108 bp read option, according to the manufacture's instruction.

Pipeline for data processing: The raw sequence data generated from Illumina GAIIx or HiSeq2000 sequencers were processed through the in-house pipeline constructed for whole-exome analysis of paired cancer genomes at Human Genome Center the Institute of Medical Science, University of Tokyo. The data processing is divided into two steps,

1) Generation of a .bam file (http://samtools.sourceforge.net/) for paired normal and tumor samples for each case.

2) Detection of somatic point mutations and indels by comparing normal and tumor BAM files.

Generation of .bam files: *Preprocessing:* First, .fastq files originally generated from Illumina sequencers are converted to .fastq in Sanger format via the maq-sol2sanger [http://maq.sourceforge.ned/]. PCR adaptor sequences contaminated in the sequence reads were removed by the following procedure: If the first 12 consecutive 3' bases of the opposite adaptor sequence were matched, the remaining bases were matched to the remaining adaptor sequence. If and only if the all the remaining sequence was completely matched, all the matched bases were removed from the read.

Mapping of sequence reads and detection of duplicate reads: Sequenced reads are aligned to the NCBI Human Reference Genome Build 37 with BWA (version 0.5.8 and default parameter settings) [http://bio-bwa.sourceforge.net/]. The output is written into a .sam file, which were converted into a .bam file format for the subsequent calculations via SamFormatConverter in the Picard suit [http://picard.sourceforge.net/Picard]. The aligned reads are examined with the MarkDuplicates algorithm from Picard to identify molecular duplicates, where a read is considered a molecular duplicate, if both ends of the pair reads are mapped to the identical genomic locations. The detected duplicates are flagged in the .bam file.

Local re-alignment: After mapping to the reference genome and detection of duplicate reads, local re-alignment was performed to increase the sensitivity and specificity of indel detection, in which the entire context of multiple mapped reads has to be taken into account and serves as evidence for putative indels. Most short read aligners map each read independently to the reference genome and hence reads supporting indels may be aligned with multiple mismatches to the reference rather than with a gap. We applied IndelRealigner in Genome Analysis Tool Kit (GATK) [http://www.broadinstitute.org/gatk] to perform multiple sequence re-alignment around the locations of candidate indels. This step tries to correct the above mentioned placement errors and decrease the false positive rate of indel and SNV calls.

Recalibration of base quality and aggregation of sample data in multiple lanes: Each sequenced nucleotide within a short read was associated with a Phred-like quality value which indicates the probability that the base call was wrong. We used GATK to recalibrate the base quality scores after the re-alignment process. The software recalculates Q scores based on the originally reported quality score, the position of the nucleotide within the read, and the preceding and current nucleotide. Finally, sequence data for the same sample from multiple lanes were combined into single .bam file using samtools-merge command [http://samtools.sourceforge.net/].

Detection of somatic mutations and indels:

Generation of the pile-up files for tumor and control data: Before summarizing base call data, low quality reads are eliminated from each .bam file, including those reads which have more than 5 mismatches to the reference sequences or whose mapping quality was less than 30 were removed. The sequence data in .bam files were then summarized into .pileup file, which contains the counts of each base call at every nucleotide position in the target sequences. To suppress too many false positive finding, the following nucleotide positions were eliminated from the further analysis, including those positions at which the depth is less than 10 in either tumor or control, or the most frequent single nucleotide variant (SNV) or indel accounts less than 7% of all reads in tumor. The SNV comprising equal to or more than 7% of total reads at each nucleotide position, if exists, is adopted as the candidate mutation.

Statistical evaluation of SNVs and indels: The significance of each candidate mutation is evaluated by Fisher's exact test by enumerating the number of the reference base and the candidate SNV in both tumor and control. Candidate mutations either (i) having p-values of less than 0.001, or (ii) having p-values of less than 0.05, more than 20% of the mutated allele in tumor sample and less than 10% of the mutated all in normal sample, were adopted as provisional candidate for somatic mutations. The provisional candidates for somatic mutations were subjected to validation using Sanger sequencing, if they do not satisfy any of the following conditions:

-SNPs registered in dbSNP 131.

-SNPs found in the1000 Genomes [http://www.1000genomes.org/] database.

-Variants on the intron region excluding splicing sites.

-Synonymous mutations.

Measurement of Telomere length

Measurement of absolute telomere length (aTL) was by QRT-PCR as described previously (O'Callaghan NJ, Fenech M. A quantitative PCR method for measuring absolute telomere length. Biological procedures online. 2011;13:3). The Cawthon method (Cawthon RM. Telomere measurement by quantitative PCR. Nucleic acids research. 2002;30:e47) for relative measurement of telomere length (TL) was modified by introducing an oligomer standard to measure aTL. Oligomer standards (Table S3) for both Tel & single copy gene (SCG) (36B4) were purchased from Integrated DNA Technologies, Inc.

QRT-PCR conditions: each reaction included 10 µL 2× SYBR Green mix (Bio-Rad), 0.5 µL each of 2.5 µM forward and reverse primers, 6.5 µL molecular-filter water and 2.5 µL genomic DNA (7 ng/µL) to yield a 20-µL reaction per well. All samples were run on an ABI 7500 Fast-real time PCR Detection System with Ver. 2.0.4 software (Applied Biosystems [AB], Foster City, CA). Reaction conditions 95°C for 10 min followed by 40 cycles of data collection at 95°C for 15 s, 60°C anneal for 30s, and 72°C extend for 30s followed by 80 cycles of melting curve from 60°C to 95°C. After thermal cycling was completed, the 7500 Fast RT PCR software version was used to generate standard curves and Ct values for telomere signals and 36B4 gene signals.

Six levels of diluted standards were analyzed to generate a standard curve using the formulas shown below (**figure S7**). This standard curve was used to to derive absolute telomere length of patient and normal control samples analyzed in conjunction with known short/long telomere controls (Roche #12209136001). Formulas:

• The synthesised 36B4 oligomer standard is 75 bp in length with a MW of 23268.1.

• The weight of one molecule of 36B4 oligomer standard is MW/Avogadro's number = $23268.1/6.02 \times 10^{23} = 0.38 \times 10^{-19}$ g.

• The highest concentration standard (SCG STD A) had 20 pg of 36B4 oligomer per reaction.

• Therefore there are $20\times10^{-12}/0.38\times10^{-19} = 5.26\times10^{8}$ copies of 36B4 amplicon in SCG STD A.

• Therefore SCG STD A is equivalent to 2.63×10^{9} diploid genome copies, because there are two copies of 36B4 per diploid genome.

A standard curve was generated by performing serial dilutions of SCG STD A (10^{-1}through to 10^{-6}dilution).

Human Telomere copy number per reaction was calculated as follows:

• The oligomer standard is 84 bp in length (TTAGGG repeated 14 times), with a molecular weight (MW) of 26667.2.

• The weight of one molecule is MW/Avogadro's number = $26667/6.02\times10^{23} = 0.44\times10^{-19}$g.

• The highest concentration standard (TEL STD A) has 5 pg of telomere oligomer (5 × 10-12g) per reaction.

• Therefore there are $5 \times 10^{-12}/0.44 \times 10^{-19} = 0.1136 \times 10^{9}$ molecules of oligomer in TEL STD A.

• The amount of telomere sequence in TEL STD A is calculated as: $0.1136 \times 10^{9} \times 84$ (oligomer length) = 95.45×10^{8} bp of telomere sequence in TEL STD A.

A standard curve was generated by performing the aTL qPCR assay on serial dilutions of TEL STD A (10^{-1} [95.45×10^{8}] through to 10^{-6} [95.45×10^{3}] dilution).

Final results were reported as aTL in base pair (bp) per genomic copy following adjustment of telomere length to the single copy gene from the same sample.

Analysis of master transcription factor expression in normal hematopoietic stem cells (NHSC), MDS stem cells (MDS-SC), and AML stem cells (AML-SC)

Master transcription factors analyzed for gene expression were HLF that drives stem cell fate and CEBPA, PU.1 and GATA1 that drive myeloid lineage-fates, demonstrated in lineage-conversion and murine knock-out studies (1, 2). Surface phenotypes defining NHSC, MDS-SC and AML-SC and used for flow-purification, reproducibly identify cell fractions with the capacity to reconstitute long-term myelopoiesis in immuno-compromised mice (3, 4)(GSE55689 and GSE24006). NHSC and MDS-SC were $DAPI^{-}Lin^{-}CD34^{+}CD38^{-/lo}CD90^{+}CD45RA^{-}$; AML-SC were $DAPI^{-}Lin^{-}CD34^{+}CD38^{-/lo}CD90^{-}$ (AML engrafting cells differ from NHSC and MDS-SC in being CD90-, and can also be CD38+, a fraction not analyzed here)(3, 4). Lineage markers analyzed included CD2, CD3, CD4, CD7, CD8a, CD10, CD11b, CD14, CD19, CD20, CD56, CD235ab, glycophorin-A and CD123. MDS and AML cases were representative of the morphologic and genetic spectrum of disease, and in the case of MDS, included low and intermediate-risk cases (3, 4). Gene expression was relative to mean expression of the same gene in simultaneously analyzed NHSC.

Data Collection and Statistical Methods

Data was collected into a protected Oncore database. The sample size (25 patients) was based on a 2-stage design with a null hypothesis of 30% of the patients having a hematological improvement versus an alternative hypothesis of 60%, using a one-sided alpha of 5% and power of 90%. After 15 patients, at least 5 hematologic improvements were needed for the trial to proceed, at which point 10 additional patients were enrolled.

Parameters related to response, mechanism-of-action and prediction of response (pharmacodynamics: DNMT1 - molecular target of therapy, γH2AX - DNA damage and cytotoxicity marker; terminal differentiation: p27/CDKN1B; proliferation/oncoprotein: MYC; growth fraction and deoxycytidine kinase surrogate: KI67) were percentages (i.e. of cells positive for a marker) and thus not normally distributed. We therefore used the nonparametric Wilcoxon Signed Rank Test to determine the significance of within-patient differences between time points. Fisher's exact or chi-squared test was used to compute P values of differences in proportions of adverse events or positive biomarkers. P values were computed using SAS9.2 (SAS Institute, Cary, NC) and R 3.0.1 (http://www.r-project.org/). p-values <0.05 are considered statistically significant.

Table S1: Mutations detected by whole exome sequencing* in responding (hematologic improvement or complete remission) subjects (Patient #s 3, 10, 14 were analyzed by targeted exome sequencing). A) Mutations in responders. B) Mutations in non-responders. Known recurrent mutations are highlighted in bold, and apoptosis genes are additionally underlined.

A) Patient#	MUTATIONS IN RESPONDERS									
1	AXIN2	DOCK8	LRP1	CDH11	**SRSF2**	**BCOR**	**JAK2**	LARP1B	GIGYF1	OVCH2
	PTPRM	MUC5B	**TET2**	CUX1	**RUNX1**	LARP1B	**ASXL1**	MUC21		
4	**TET2**	**KDM6B**	PTPRZ1	GPR107	FMN2	**TP73**	**SF3B1**	LAMA2	DYNC2H1	BCORL1
	ANPEP	MUC16	**BCOR**	**CEBPA**	DHX29	**DNMT3A**	**KDM6A**	**RUNX1**	**SRSF2**	**SUZ12**
	ABCB1	ABCC3	ABCF3	ACSF3	ADCY5	ADRA1B	AKAP13	ANO7		
	AP3B2	APC2	ARHGEF2	ASPA	ATP13A3	AXDND1	B3GALT4	B4GALNT3	B4GALNT4	BMP2K
	C10orf129	C17orf64	C19orf21	C22orf43	CCDC48	CCDC64	CCDC87	CDC23	CDH11	CDH16
	CDON	CEP78	CHST10	CLASP1	CLCN6	CMYA5	CNTN6	COL27A1	COL2A1	COL4A1
	COL4A6	COQ3	CREB3L4	DCP2	DCTD	DDX6	DENND1C	DGKD	DLG2	DNAH3
	DNAJC25	DOCK10	DPF1	DSC3	DSE	ZZEF1	ECHDC3	EIF4E3	EMP3	EPHB2
	EPHB6	ERN1	FAM194B	FAM194B	FAM194B	FAT2	FBLIM1	FCHO1	FHDC1	FRY
	FRYL	FZD5	GAK	GAS1	GEMIN5	GFM2	GPR158	GPR84	GPRIN3	GTF2IRD1
	HBS1L	HEATR5A	HEATR5B	HECTD4	HERC2	HMHA1	HSPBAP1	HTATIP2	IGSF10	IL1RAP
	IL20RA	INCENP	IRX2	ITSN1	KIAA0196	KLF9	KLHL36	KPNB1	KRTAP4-3	
	LAMA4	LAMB4	LARP7	LIG4	LONRF3	LPAR2	LRP2	LRP2	LRRC34	LTK
	LTN1	MAEL	MAN2B2	MDGA1	MMEL1	MPDZ	MRGPRF	MSMO1	MST4	MUTYH
	MYBPC1	MYH1	MYH14	NAPRT1	NKAIN2	NOA1	ODF3L2	OLFML2A	OR1G1	
	OR5M8	OR9G4	PCDH1	PCDHGA6	PCED1A	PCMTD1	PCNX	PCNXL4	PDE9A	
	PELI2	PHIP	PIK3R5	PIKFYVE	POLI	PPARGC1B	PPP6R2	PRMT7	PSME4	PTPRM
	RAB11B	RAD18	RBBP8	RFWD2	RHBDF2	RNF149	RNF170	RNF6	RNGTT	RUNX1T1
	SBF2	SCFD1	SDC2	SEC23IP	SEC24B	SERPINB8	SGIP1	SHROOM3	SIX4	SLC2A10
	SLC4A5	SLC9C2	SMPD3	SMYD1	SOGA3	SP140	SPATA6	SPTB	ST5	
	STK36	SUPT3H	TAAR5	TBC1D13	TCF20	TECRL	TENM4	THADA	TMEM131	
	TMEM244	TPP2	TRANK1	TTBK1	ULK4	URB1	UROC1	VPS13A	VPS37A	VPS37C
	VPS4B	WDFY3	WDR66	WNT3A	WSB1	XIRP1	ZC3H4	ZCCHC14	ZNF140	ZNF182
	ZNF605	ZNF717	ZNF814	ZNF830	ZNF880					
8	STXBP4	LYST	PUS10	ATN1	MUC6	ALMS1	INTS9	ZNF516		
9	C8orf59	FOLH1	GJA3	FSIP2	**ATM**	SSX4B	SLIT2	**SRSF7**	**MLL2**	**ARID2**
	ORC2	**TET2**	C10orf76	DRD2	OR10Z1	BCL11B	CNTNAP2	KRAS	OR10Z1	
	PCDHA13	**SRSF2**								

11	RAN	SACS	**TP53**	FRMD3	ANKRD20A4	MDN1	SAA1	ODZ1	CMYA5	
	TPBG	GNL3	MPP5	NSUN7	CTNNA2	CADPS2	RNF123	CCDC123	CDON	EIF3A
	PCMTD1	CORO7	ZNF208	HAVCR1	MEP1A	TXLNA				
13	HYDIN	STRN4	PRSS3		FST	MUC17	TAF2	SYNPO2	KRTAP5-2	
	RPL14	TTN	PCDHB9	IQGAP3	PCDH17	CCNE1	C14orf21	NOS1	PLA2G4F	EI24
	OR14A16	**KDM4B**	CD97	MTMR4	SLC15A3	SYNE2	**BCOR**	HLCS	PCCA	
	ARHGAP36	ARMC4	B3GAT3	**BCL11A**	C12orf51	C12orf77	C3orf59	C7orf43	CACNA1E	
	CACNA2D3	CASKIN2	DNAH6	EFCAB6	EI24	**ETV6**	PDE6C	FAM83H	**EZH2**	
	FAM82A2	FCGBP	FGD2	CLTB	FRS3	GPR109B	GPR55	GPR97	HBM	ITPKC
	KCNH7	USH2A	KLHL26	UBAP2L	MAPK8IP3	MED12	MICAL3	MSR1	WNK2	
	OGT	PAK6	PASD1	PCDHA4	PDCD6	PDE11A	PIKFYVE	PLD2	PLEKHG4	
	PPFIA2	**U2AF1**	RGS3	SNIP1	STK10	TSHZ1	TAF15	TLN2		
14	**SF3B1**									
17	ALDH3B1	HCFC1	CHD7	**FASLG**	MUC17	KIAA0562	FRRS1	CRYAB	HCN2	ZNF814
	MASP1									
18	ADCY2	BCAM	UPB1	CRMP1	PRDM14	FMO2	ZNF248	PTPRU	SCIN	ZAK
	OR8I2	C8B	**TET2**	TRIML2	LNX1	ASH2L	**CBL**	APOBEC3D	**SRSF2**	C15orf23
	AKR1E2	CYP2E1	FGD2	CCDC50	SIPA1	MICALCL	GDPD4	CEBPZ	AURKA	
	POLG	NLRP11	NOTCH4	AUTS2	KLB	CAMTA2	COL7A1	CAMK1	CLDN7	LARP7
	MCM3AP	PRPF8	PTTG1IP	SETD1B	SLC22A9	**TP53AIP1**	TRIM16	TUB	UPK2	WDR46
	ZNF282	KIAA0415	LRRC3B	ABCB10	ACSM2A	ADCK5	ADCY5	AOC3	ARHGEF25	ARL13B
	ARNT	ARSD	ATP9A	BCOR	C16orf45	C19orf61	C3orf64	C3orf75	CAPN2	CARS
	CD164	CHRM5	CHRNE	CNKSR2	CNPY3	CNTROB	COL4A1	CSAD	CSPG4	
	CTU2	**DDX5**	DIP2C	DLX1	DNAH17	DNAH9	DNAJB12	DNAJB6	DPYD	DSG3
	DYSF	EFEMP2	EHMT1	EIF2B5	ELL2	ELMO3	FA2H	FSIP2	GALNT10	GALNTL2
	GGT7	GLI2	GRIK3	GTF2IRD1	HK2	HMG20B	ICAM3	IGDCC3	IGSF21	IL11RA
	IL1R2	IRX1	KIAA0664	KIAA0947	KIAA1161	KIAA1407	KIAA1797	KIF26B	KLHL31	KLHL33
	LRFN5	LRRC16A	LYZL4	MAN2B2	MAOA	MAPK7	MFN1	MUC2	MYO19	MYO9A
	MYSM1	NBEAL2	NLE1	NOTCH4	NXF5	OGG1	OPRL1	OR11H6	OR7G2	OSTN
	PEAR1	PGS1	PHF1	PIK3CB		PLEKHH1	PLK1S1	PRDM4	PSMC1	PTH1R
	PTX4	RACGAP1	RBM26	RGNEF	RGS9	**RUNX1**	SATB1	SDCBP2	SH3YL1	SLC25A13
	SLC25A41	SLC5A10	SLC6A20	SLIT2	SPC24	SRRM1	STRA6	THOC2	THOC2	TMEM194B
	TMEM63A	TNFSF15	TRAF3IP2	TRMT1	TSPAN6	UBTF	UGT3A2	UHRF1BP1L	UTP3	WDR87
	ZCCHC5	ZFAND6	ZFYVE27	ZNF687	ZNF775	ZSCAN21	CD300A	CLSTN3	COL14A1	**KDM6B**
	KIAA0355	KIAA1467	PRDX2	SIGLEC6	TBRG4	TMEM110				

19	TRIM65	HIP1	HAVCR1	PLXNC1	FST	ATP1B4	SLC12A1	FHAD1	TMEM216	ACTR1B
	MC4R	MUC2	NMT1	SEBOX	TBC1D9	VCX3A				
21	MUC2	MUC5B	SERPINB12	DNAH10	AR	ADCK5	AFAP1	CYP1A2	FRMD4A	IRF2BP1
	LRP2		TCF12	TMEM63A	TSNARE1	TWSG1	ZNF157			

B) Patient#	MUTATIONS IN NON-RESPONDERS									
2	CCDC144NL	DNMT3B	AKAP12	USP35	KIF20B	PCLO	RAI14	PCLO	APOBEC3H	
	LRRC31	CD97	CDC20B	MYRIP	ATP2C2	ZNF814	APOBEC3H	SH2D5	CSMD1	NOX4
	AOC3	ERBB4	GRK6	ITGBL1						
3	**SF3B1**									
5	CLCN7	ARHGAP36	GSPT1	PPRC1	**ASXL1**	TNPO2	C12orf56	SEMA3F	RAPGEF5	
6	**PHF6**	ATP6V0C	KPRP	FHDC1	PHF10	SLC4A4	MAP3K4	CCDC135	SPTAN1	HOXA13
	DDX54	RBM6	DEFB118	NPY1R	CDH11	**TP53BP1**	TRIOBP	**SF3B1**	L1CAM	TSPAN11
	HNRNPK	ABCD4	FBXL21	TTN	CELF2	SLC25A3	ARC	**FLT3**	FMNL1	IMPG2
	KCNA5	KCNT2	KIAA1409	PCDHA1	PHOX2B	PPFIA2	PWWP2B	**RUNX1**	STS	SYT14
	VPS8	WSCD1	WT1							
7	VEZF1	MUC2	**SF3B1**	DNMT3B	PCDH8	MTNR1B	ZNF717	TRIOBP	ADRBK1	CLDN8
10	**ASXL1**	**PRPF8**	**TP53**							
12	FAM71E2	ABLIM1	C9orf79	KIAA1257	MIR205HG	MUC16	PAX5	ZFP36L2		
15	EHD3	FRG1	ANKRD30A	PCDHA4	ERCC6	NUPL1	RRP9	**IDH1**	NCAPG	KIAA1244
	TWSG1	AMELY	COL19A1	GLMN	NT5C1B	ROCK2	VPS36	ZFP64	DLAT	**NPM1**
	POLG	ABCA9	ALDH3B1	ARHGEF15	C1orf9	C1QTNF3	CCDC152	CENPB	COL19A1	CYLC2
	DMXL1	DNAH12	DYNC2H1	ESYT2	**FLT3**	GFRAL	GMCL1	GNL2	GTF2H2	HDAC9
	IDE	ITSN2	KRIT1	LPHN1	MAN1A1	MYH14	NKAP	NUPL2	OBFC2A	PIGB
	RPGRIP1L	SI	**SRSF2**	STAB2	**SUZ12**	SYNE2	TBC1D8B	THY1	TTC14	UBE2H
	UBE2U	USP25	UTP15	UTS2D	ANKRD18A	CLGN	SKA3	STAG1	STXBP5	TRPM7
	ZNF814	ATP2B2	SEC22B	ACACA	PCDHA4	NUPL1	TAF7L	RRP9		
	NCAPG	MEGF10	C11orf30	KIAA1244	FGFRL1	POLG	EMD	GEMIN7	MUC2	
16	HCRTR1	ZNF865	EXTL1	GJB4	**SRSF2**	ODZ3	SPAG17	USP8	WDR47	IST1
	DENND4B	MAGED1	STC2	SPATA21	USP38	ACTRT2	DLX6	DUSP13	FOXS1	GGT5
	KCNU1	KREMEN1	LCE4A	MTFR1	PAPLN	RPGR	STARD9	UTS2R	VARS	ARMC8
	ELMO2	SPATA21	GPR126							
20	CASP8AP2	MUC4	SERPINE3	MUC2	CLTCL1	MLC1	BAHD1	EFCAB11	LAMA3	MARS
	MTMR11	NOTCH1	SERINC2	SIRT7	SLC29A2	USP5	YIPF5	ZBTB16		
22	**SF3B1**									
23	TRAP1	C6orf163	MUC2	TRABD	C8orf86	LYRM7	TTLL2	BTBD7	PSMC5	ETFA
	GPR183	OBSCN	HEY2	ANGPTL3	POU4F2	NOS3	PPM1D	CRTAC1	CSHL1	LENG9
	RNGTT									
24	DLC1	ZNF720	BOC	ZNF596	AFF2	FBXO25	C10orf137	BRWD3	**DNMT3A**	PROZ

	FAN1	ARHGAP6	BBS7	LY9	RBM12	BOLL	SLMO1	TTK	BCHE
	KDM6B	GTPBP1	C9orf153	C15orf40	**CBFA2T3**	FPGS	MUC21	NOP16	PLEKHA7
	RNF145	SYN1	VAV2	ZNF208	CDK12				
25	**TET2**	**ATM**	**SRSF2**	KIAA0754	POLR2A	SLC5A1	UNC5D	ZCCHC11	ZNF717

Table S2: Biomarker quantification by ImageIQ software of whole tissue sections. Raw data for **A) DNMT1. B) p27/CDKN1B. C) MYC**.

A)

DNMT1	Week 0			Week 6		
Pt ID	P. Nuclei (n)	T. Nuclei (n)	Mean (%)	P. Nuclei (n)	T. Nuclei (n)	Mean (%)
Pt 1	1125	17715	7	2852	25977	13
Pt 2				1377	13913	11
Pt 3	9212	35058	25	4201	16631	24
Pt 4	8050	23036	34	9043	25547	35
Pt 5	3715	17592	20	2779	21305	12
Pt 6	870	9745	9	243	2532	9
Pt 7	30869	62147	49	9627	32440	30
Pt 8	3246	18825	17			
Pt 9	12203	34781	34	751	7594	7
Pt 10	9525	40639	16	403	6734	8
Pt 11	17169	65065	26	7826	32320	25
Pt 12	50	1095	6	572	14680	4
Pt 13	13473	43431	31	1421	9285	19
Pt 14	8381	20224	39	3033	36999	9
Pt 15	8502	31774	27	103	1198	9
Pt 16				3283	28310	11
Pt 17	3720	21949	17	1313	5020	26
Pt 18	33745	53547	63	3794	17829	21
Pt 19	9191	26055	35	3120	31330	11
Pt 20	1000	8467	14			
Pt 21	13221	24261	55	1027	9269	11
Pt 22	1156	5793	18	1812	39710	4
Pt 23	8220	30135	28			
Pt 24	13206	44381	29	4561	25865	18
Pt 25	1444	8915	17	2697	17122	17

B)

p27	Week 0			Week 6		
Pt ID	P. Nuclei (n)	T. Nuclei (n)	Mean (%)	P. Nuclei (n)	T. Nuclei (n)	Mean (%)
Pt 1	1697	10738	15	4044	14960	29
Pt 2	1614	6660	25	522	5127	10
Pt 3				206	1047	18
Pt 4	964	28929	3	4497	23668	20
Pt 5	4839	19226	25	2322	15430	13
Pt 6	8935	31894	27	51	1088	4
Pt 7	7960	50294	16	11024	26866	41
Pt 8	1766	11501	14			
Pt 9	771	35307	2	458	6099	9
Pt 10	1625	11002	16	704	5224	13
Pt 11	2495	29635	8	2326	13809	17
Pt 12	114	1281	11	128	1390	8
Pt 13	6526	48763	13	1543	7566	23
Pt 14	3803	30932	12	3304	24630	14
Pt 15	1184	33173	4	358	4510	7
Pt 16	2212	24776	9	5150	47943	11
Pt 17	3392	29826	11	1347	5287	19
Pt 18	6473	63348	10	705	18142	4
Pt 19	2325	24425	9	4765	22709	20
Pt 20	1205	13619	9			
Pt 21	8013	44375	18	970	11766	8
Pt 22	6303	46212	14	621	25394	2
Pt 23	1797	19806	9			
Pt 24	5404	43851	12	2699	22195	12
Pt 25	416	9451	4	1961	14966	15

C)

c-MYC	Week 0			Week 6		
Pt ID	P. Nuclei (n)	T. Nuclei (n)	Mean (%)	P. Nuclei (n)	T. Nuclei (n)	Mean (%)
Pt 1	351	10853	4	1532	16795	10
Pt 2	2820	9752	29	1407	6547	22
Pt 3	4715	29492	16	4171	24613	17
Pt 4	8356	39282	21	5463	22334	23
Pt 5	6864	52204	14	4217	37054	12
Pt 6	14759	59546	24	882	6403	15
Pt 7	17349	95228	18	5968	42331	14
Pt 8	2262	16386	14			
Pt 9	5605	56505	13	203	4346	5
Pt 10	3047	11053	27	471	5381	7
Pt 11	7116	37463	19	1780	13420	13
Pt 12	133	1334	14	219	7318	4
Pt 13	3401	34863	10	558	5315	11
Pt 14	4304	37148	12	1824	17169	11
Pt 15	3483	46207	8	1521	12951	13
Pt 16	1348	26751	5	3409	53373	6
Pt 17	2113	38863	6	2	1997	0
Pt 18	14327	63385	22	524	10568	5
Pt 19	2565	29327	9	1848	20796	9
Pt 20	1603	18200	9			
Pt 21	5405	58582	9	340	7887	4
Pt 22	5020	48431	10	147	12474	1
Pt 23	1406	18071	8			
Pt 24	3998	57146	7	1598	17917	9
Pt 25	819	9198	10	636	9769	9

Table S3: Oligomer standards used for absolute telomere length measurements

Oligomer Type	Oligomer Name	Oligomer sequence (5'-3')	Amplicon size
Standards	Telomere standard	**(TTAGGG)14**	**84 bp**
	36B4 standard	**CAGCAAGTGGGAAGGTGTAATCCGTCTCCACAGACAAGGCCAGGACTCGTTT GTACCCGTTGATGATAGAATGGG**	**75 bp**
PCR Primers	teloF	**CGGTTTGTTTGGGTTTGGGTTTGGGTTTGGG TTTGGGTT**	**>76bp**
	teloR	**GGCTTGCCTTACCCTTACCCTTACCC TTACCCTTACCCT**	
	36B4F	**CAGCAAGTGGGAAGGTGTAATCC**	**75bp**
	36B4R	**CCCATTCTATCATCAACGGGTACAA**	
Oligomer Type	Oligomer Name	Oligomer sequence (5'-3')	Amplicon size
Standards	Telomere standard	**(TTAGGG)14**	**84 bp**
	36B4 standard	**CAGCAAGTGGGAAGGTGTAATCCGTCTCCACAGACAAGGCCAGGACTCGTTT GTACCCGTTGATGATAGAATGGG**	**75 bp**
PCR Primers	teloF	**CGGTTTGTTTGGGTTTGGGTTTGGGTTTGGG TTTGGGTT**	**>76bp**
	teloR	**GGCTTGCCTTACCCTTACCCTTACCC TTACCCTTACCCT**	
	36B4F	**CAGCAAGTGGGAAGGTGTAATCC**	**75bp**
	36B4R	**CCCATTCTATCATCAACGGGTACAA**	

A

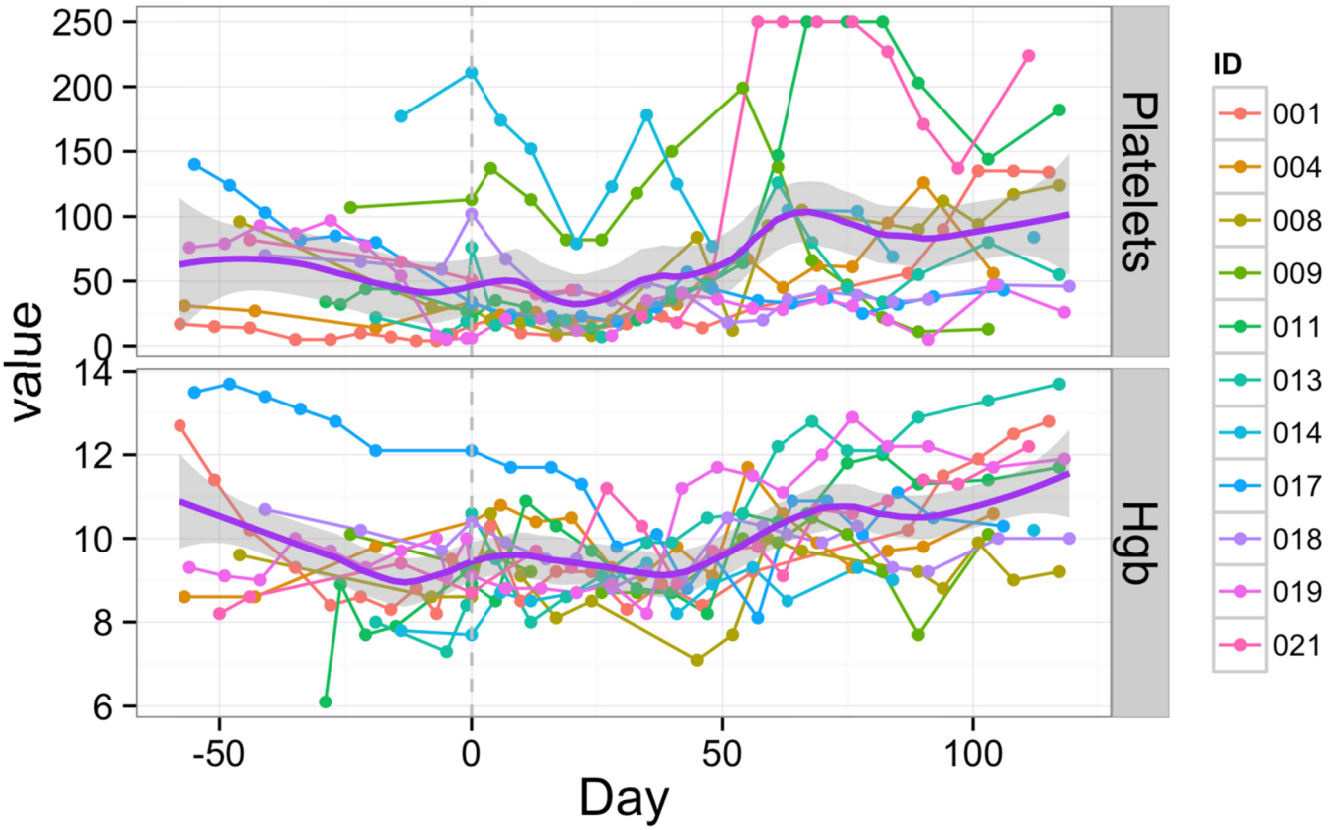

B

Subject ID	Day until which Transfusions Required	Day of Relapse/Resumption Regular Transfusion	#Days Transfusion-Free
Red Cells			
001	56	1208	1152
008	94	1049	955
011	42	359	317
013	25	315	290
014	57	308	251
017	49	NA	1106*
019	32	NA	1055*
021	13	447	434
Platelets			
001	39	1107	1068
004	18	204	186
013	25	343	318
017	1	NA	1155*
019	88	NA	999*

Figure S1: A) Hemoglobin and platelet counts 50 days prior to initiation of protocol treatment (day -50) until day +120 in 11 responding subjects. Mean values = purple line; 95% confidence interval = grey shade. Pre-study blood counts shown according to availability in study documents. Platelet and absolute neutrophil count (ANC) values x10^9/L. Hemoglobin (Hgb) values g/dL. Values were clipped if they exceeded the depicted Y-axis scales. **B) Day until which transfusions were required after initiation of treatment, and day of relapse requiring resumption of transfusion, in responders who required transfusion prior to initiation of protocol therapy.** NA and *=transfusion-free at time of analysis.

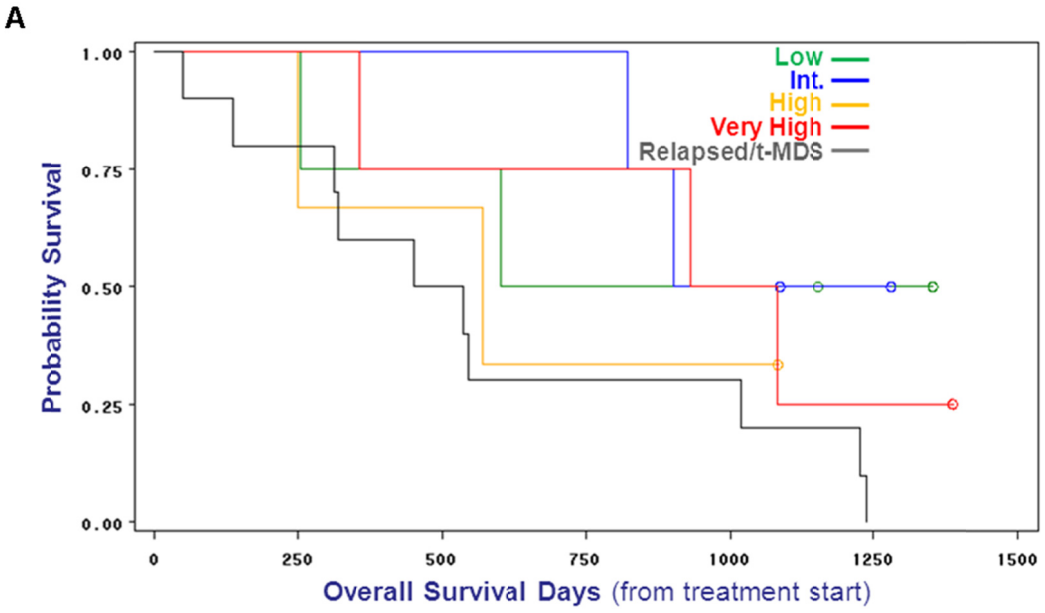

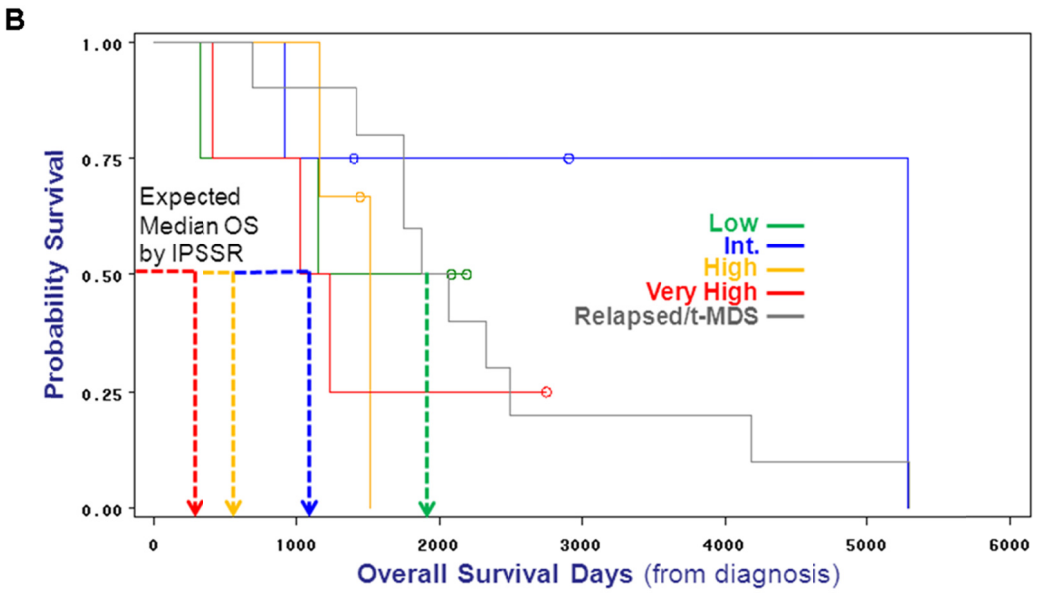

IPSS-R	Number	Deaths	Exp. mOS (years)	Obs. mOS (years)
Very Low	0	-	-	-
Low	4	2	5.3	Not reached
Intermediate	4	2	3.0	14.5
High	3	2	1.6	4.14
Very High	4	3	0.8	3.09
Relapsed/t-MDS	10	10	-	5.38

Figure S2. Observed versus Expected Overall Survival by IPPS-R risk categories. **A) From start of treatment on this protocol**. No subjects were in the IPSS-R very low risk category. Patients with relapsed or therapy-related MDS (t-MDS) were not analyzed in the IPSS-R. **B) From time of diagnosis**. Dashed vertical arrows indicate expected median 3 year survival per IPSS-R risk categories (5). Exp. mOS = expected median overall survival; Obs. mOS = observed median overall survival.

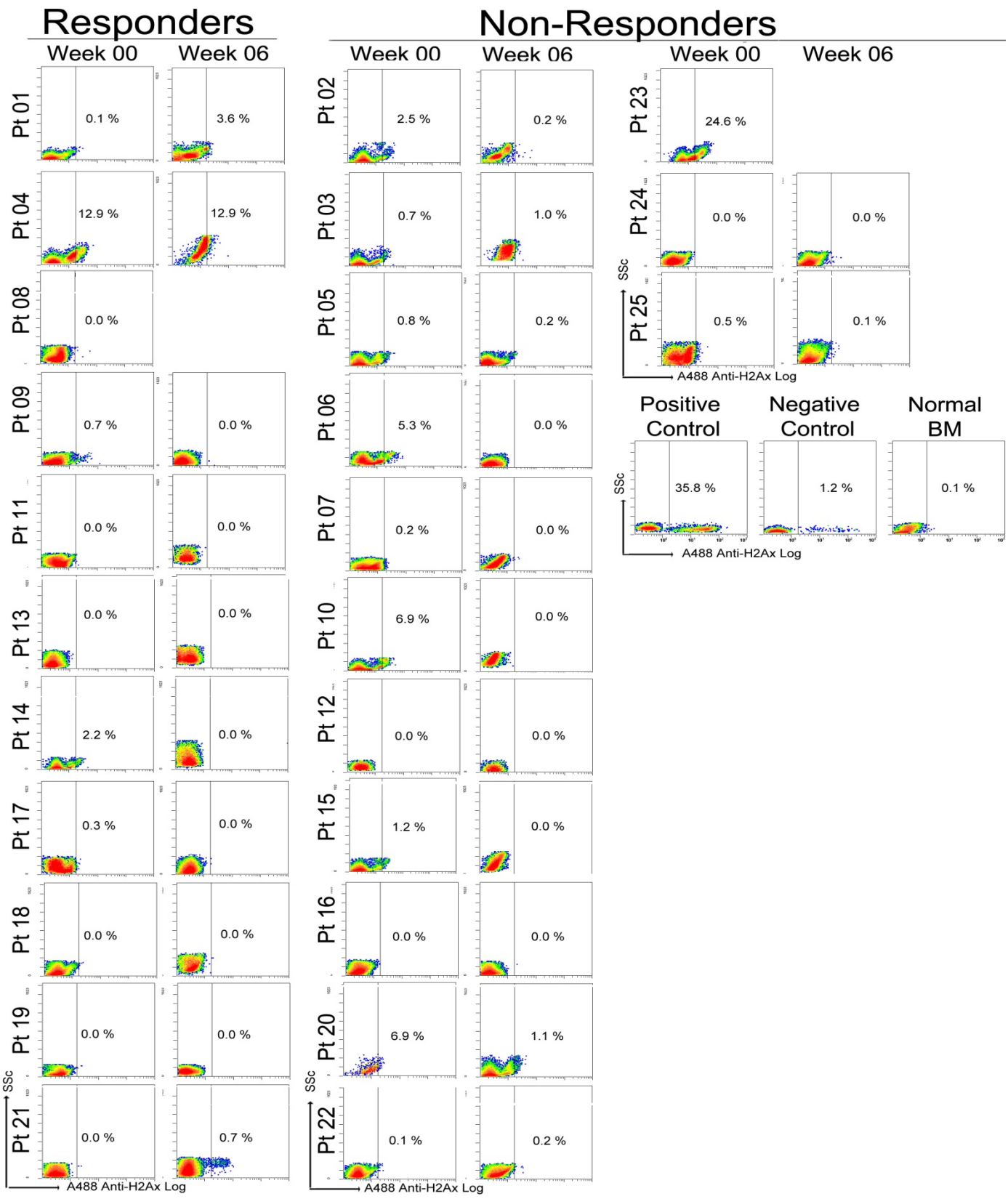

Figure S3: Flow cytometric quantification of γH2AX in bone marrow cells prior to treatment (week 0) and after 6 and 12 weeks of therapy in responders versus non-responders (per IWG criteria). Positive and negative control cells (Cat 51-6553LZ) as well as healthy donor cell controls were concurrently stained and analyzed. Flow cytometric analysis was performed with an FC500 flowcytometer (Beckman-Coulter Inc) equipped with CXP acquisition software (CXP analysis 2.2, Beckman Coulter Inc). Gating was determined by positive and negative controls, and results were expressed as the percentage of cells demonstrating fluorescence intensity located within this positive gate.

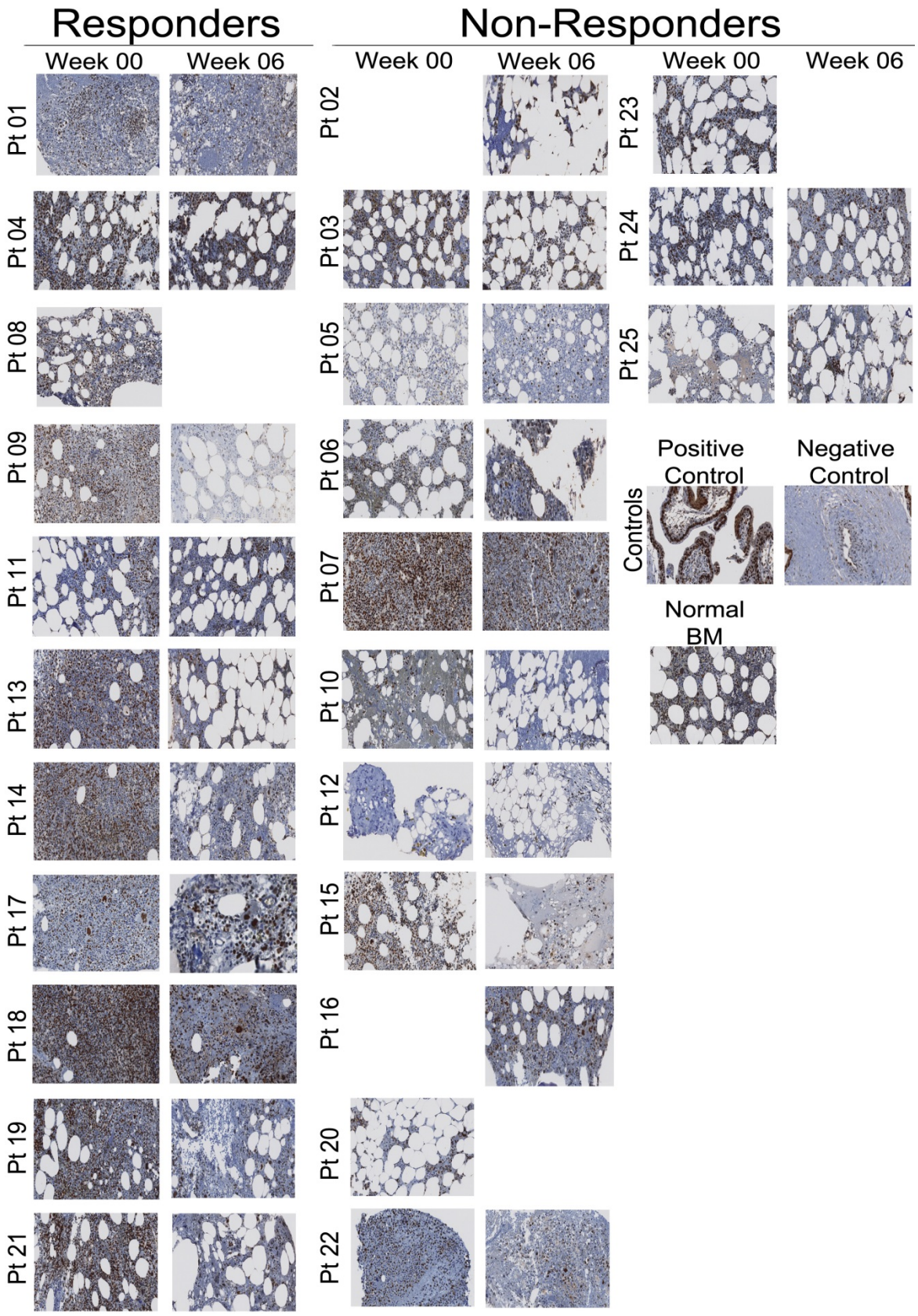

Figure S4. DNMT1 protein expression decreased during treatment. Decalcified and formalin-fixed paraffin embedded sections (4 µm) of bone marrow biopsies from different time points were concurrently immuno-stained on the same slide (raw data for all subjects in supplementary material), and on positive and negative controls. ImageIQ software was used to segment the image and positive nuclei were objectively quantified in cellular segments. Raw data from software quantification of positive nuclei is in Table S2. Examples of quantified segments are shown.

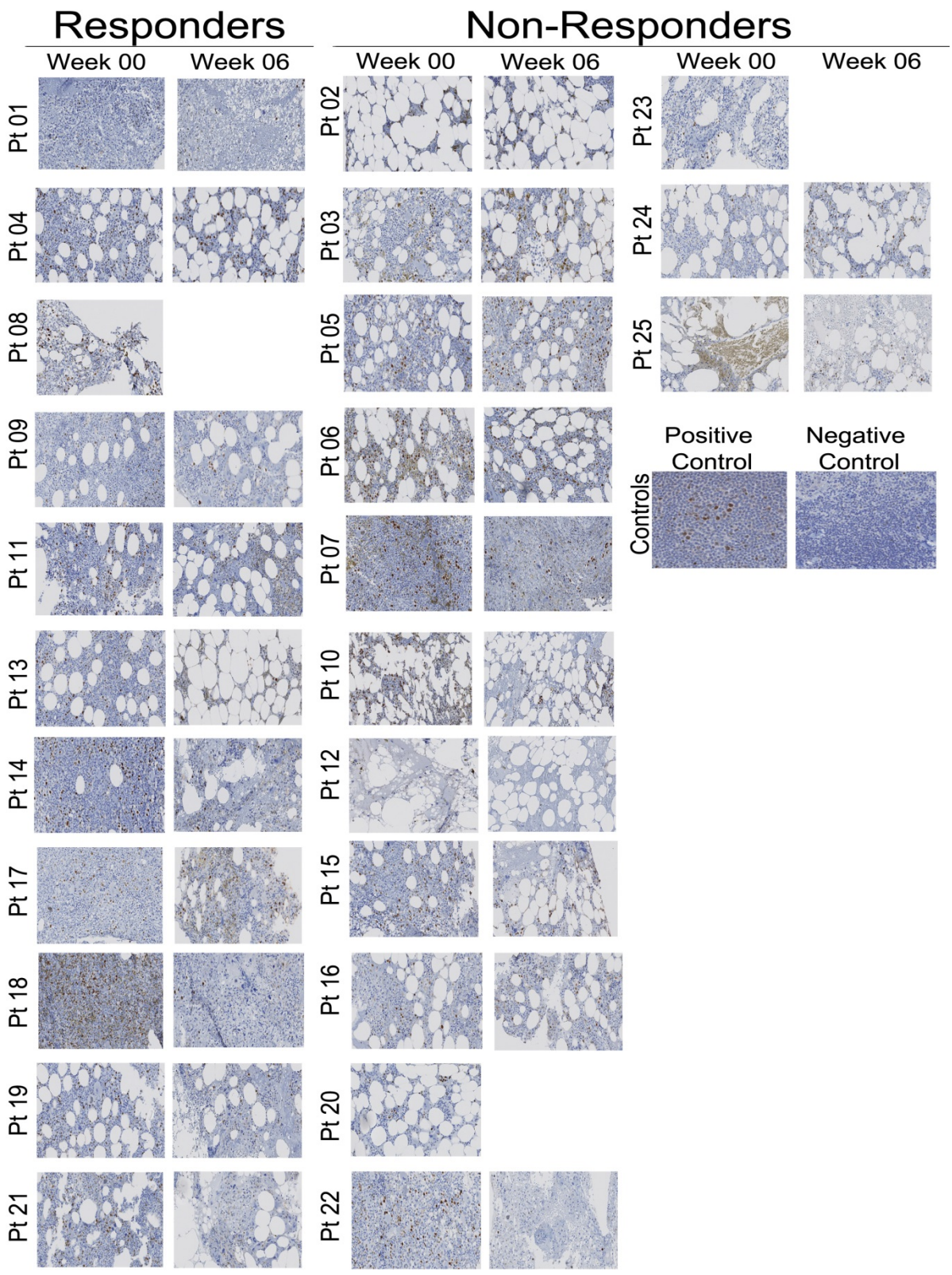

Figure S5. MYC protein expression decreased between week 0 to 6. Decalcified and formalin-fixed paraffin embedded sections (4 µm) of bone marrow biopsies from different time points were concurrently immuno-stained on the same slide (raw data for all subjects in supplementary material), and on positive and negative controls. ImageIQ software was used to segment the image and positive nuclei were objectively quantified in cellular segments. Raw data from software quantification of positive nuclei is in Table S2. Examples of quantified segments are shown.

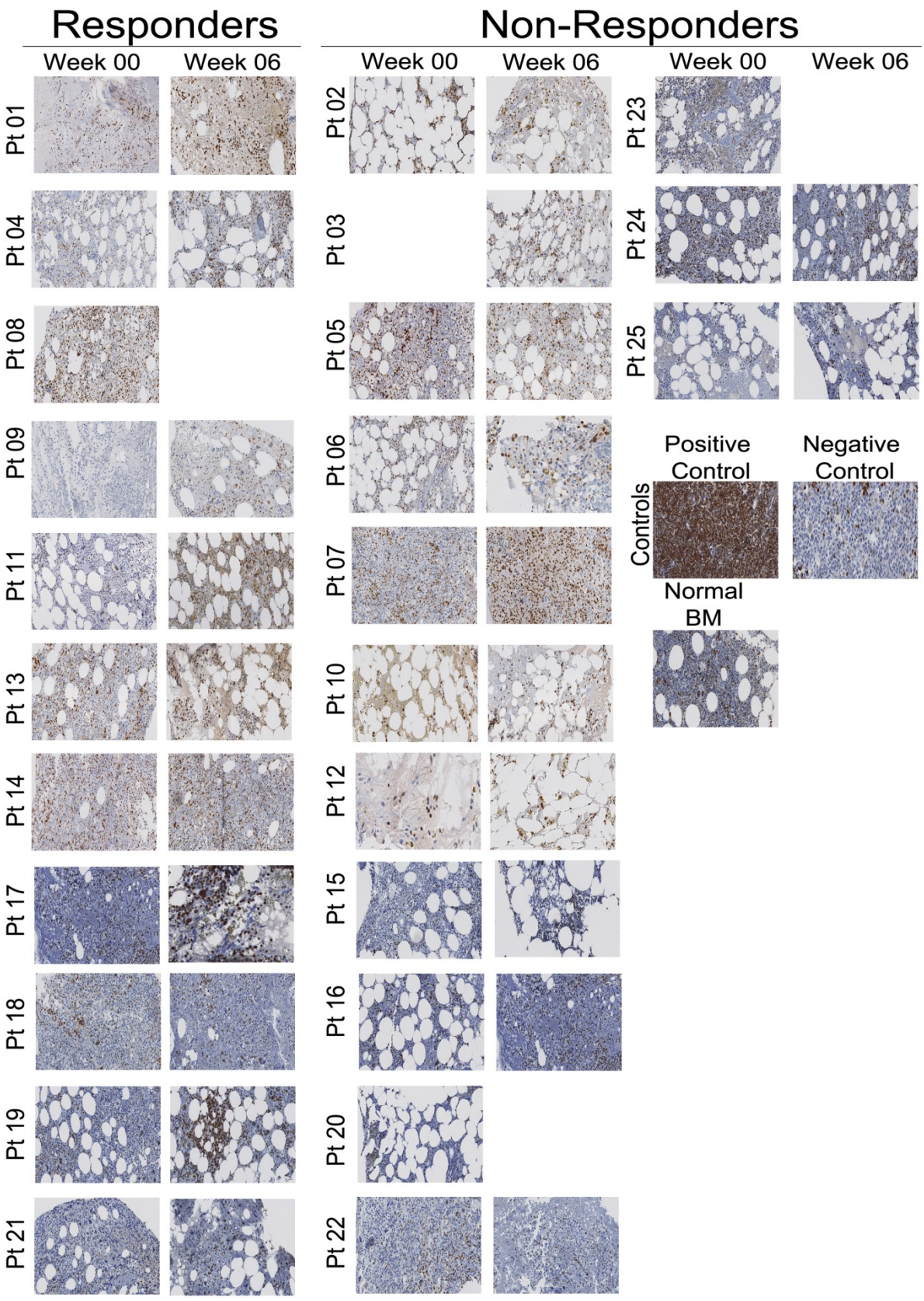

Figure S6. p27/CDKN1B protein expression increased between week 0 to 6. Decalcified and formalin-fixed paraffin embedded sections (4 µm) of bone marrow biopsies from different time points were concurrently immuno-stained on the same slide (raw data for all subjects in supplementary material), and on positive and negative controls. ImageIQ software was used to segment the image and positive nuclei were objectively quantified in cellular segments. Raw data from software quantification of positive nuclei is in Table S2. Examples of quantified segments are shown.

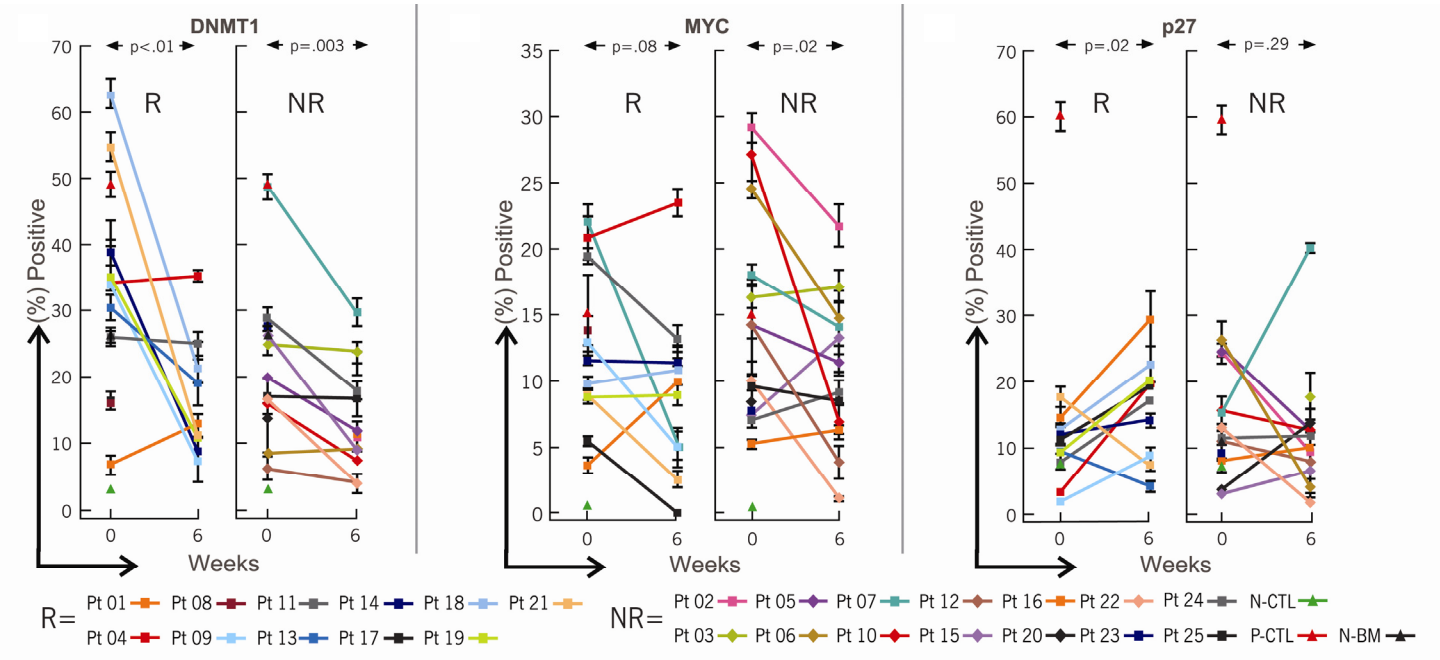

Figure S7. Changes in DNMT1, MYC and p27/CDKN1B protein expression between week 0 to 6 in individual subjects. R=responders. NR=non-responders. Graphical representation of raw data represented in Figures S3- S5. Decalcified and formalin-fixed paraffin embedded sections (4 µm) of bone marrow biopsies from different time points were concurrently immuno-stained on the same slide (raw data for all subjects in supplementary material), and on positive and negative controls. ImageIQ software was used to segment the image and positive nuclei were objectively quantified in cellular segments (shown are mean values±standard deviation for multiple segments for each patient and time-point). Raw data from software quantification of positive nuclei is in Table S2. Positive, negative and normal bone marrow controls as indicated. p-value paired t-test.

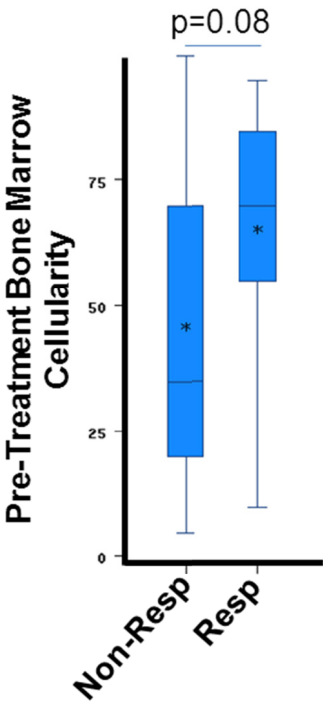

Figure S8. Pre-treatment bone marrow cellularity was higher, but not statistically significantly, in responders than non-responders. Estimated by clinical pathology pre-treatment (prior to treatment and response determination). p-value Mann-Whitney test.

Figure S9. In AML patients, there was a significant inverse correlation between presenting platelet and white blood cell counts (TCGA, n=196). Pearson correlation coefficient.

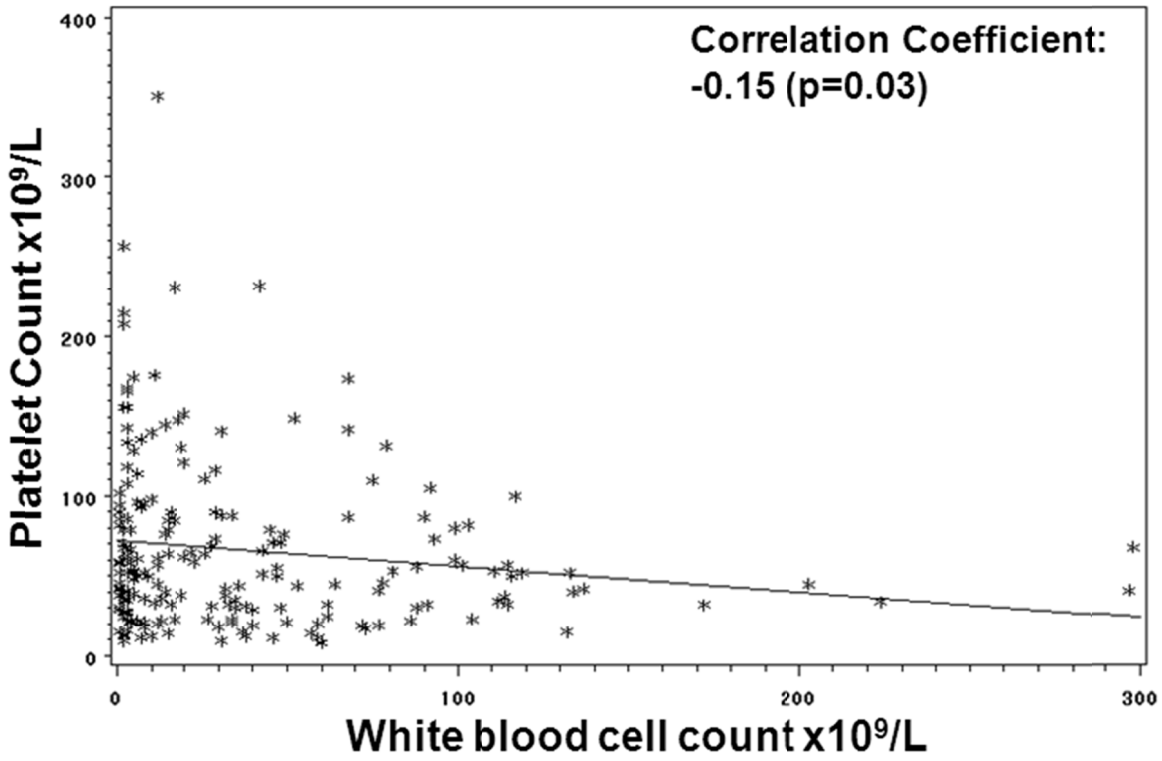

Figure S10. Standard curve used to calculate absolute telomere length.

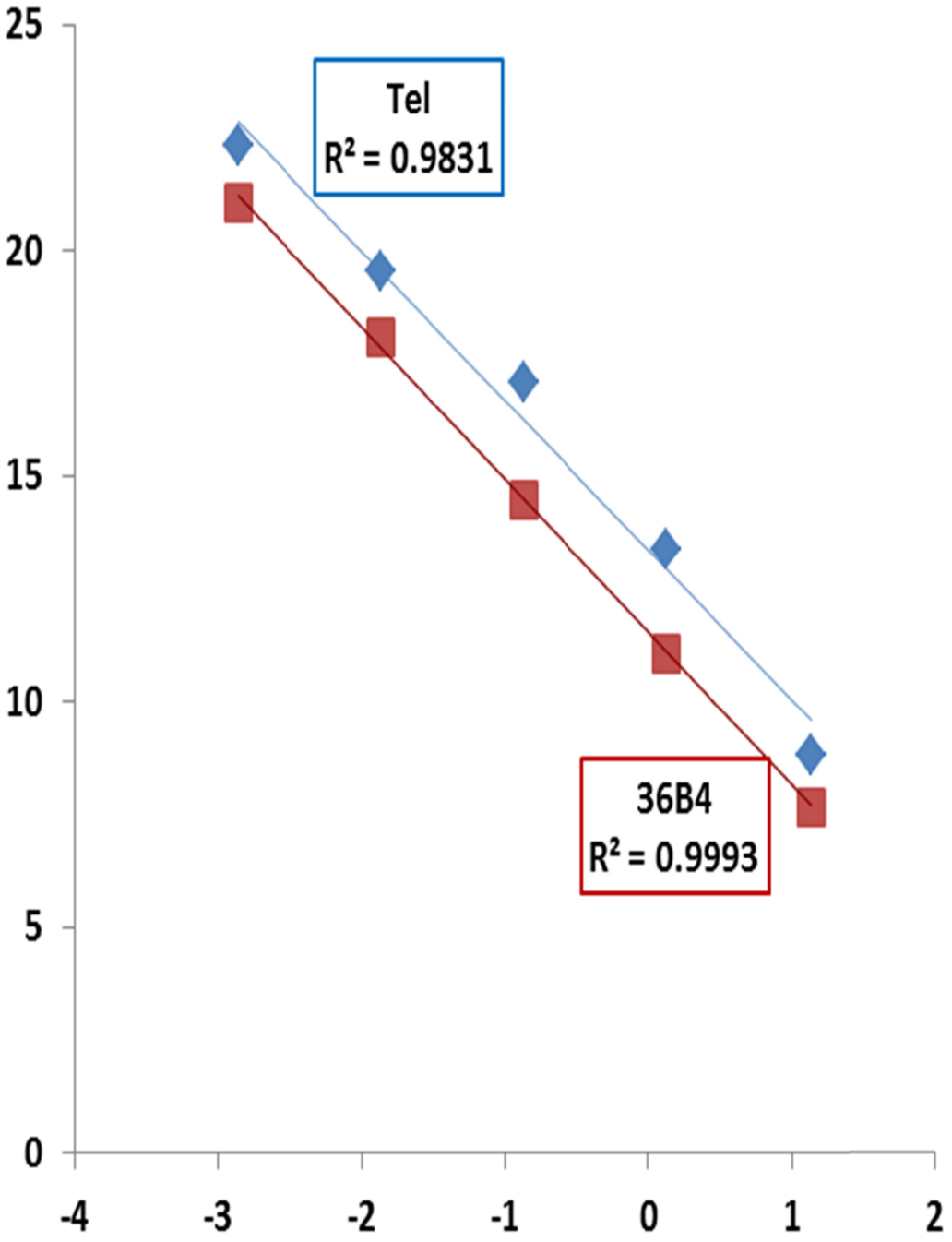

REFERENCES CITED IN SUPPLEMENTARY MATERIAL

1. Vierbuchen T, and Wernig M. Molecular roadblocks for cellular reprogramming. *Mol Cell.* 2012;47(6):827-38.
2. Riddell J, Gazit R, Garrison BS, Guo G, Saadatpour A, Mandal PK, Ebina W, Volchkov P, Yuan GC, Orkin SH, et al. Reprogramming committed murine blood cells to induced hematopoietic stem cells with defined factors. *Cell.* 2014;157(3):549-64.
3. Woll PS, Kjallquist U, Chowdhury O, Doolittle H, Wedge DC, Thongjuea S, Erlandsson R, Ngara M, Anderson K, Deng Q, et al. Myelodysplastic Syndromes Are Propagated by Rare and Distinct Human Cancer Stem Cells In Vivo. *Cancer Cell.* 2014.
4. Gentles AJ, Plevritis SK, Majeti R, and Alizadeh AA. Association of a leukemic stem cell gene expression signature with clinical outcomes in acute myeloid leukemia. *JAMA.* 2010;304(24):2706-15.
5. Greenberg PL, Tuechler H, Schanz J, Sanz G, Garcia-Manero G, Sole F, Bennett JM, Bowen D, Fenaux P, Dreyfus F, et al. Revised international prognostic scoring system for myelodysplastic syndromes. *Blood.* 2012;120(12):2454-65.